Investigation of the phase structure of poly(D(−)3-hydroxybutyrate)/atactic poly(methyl methacrylate) blends by small-angle X-ray scattering

M. Canetti*, P. Sadocco, A. Siciliano and A. Seves
Stazione Sperimentale per la Cellulosa, Carta e Fibre Tessili Vegetali ed Artificiali, Piazza L. da Vinci 26, 20133 Milano, Italy
(Received 9 August 1993; revised 17 January 1994)

Blends of poly(D(−)3-hydroxybutyrate) (PHB) and atactic poly(methyl methacrylate) (aPMMA) were isothermally cold-crystallized from homogeneous amorphous samples obtained by quenching. X-ray techniques were employed to investigate the phase structure of the cold-crystallized blends. The long period distance and the amorphous interlamellar distance increased with increasing aPMMA content in the blends, while the thickness of the crystalline lamellae was quite constant for the blends, and higher than for pure PHB. These results indicate that during isothermal cold-crystallization the aPMMA component is segregated in the amorphous PHB interlamellar regions.

(Keywords: poly(hydroxybutyrate); poly(methyl methacrylate); blends)

Introduction

The miscibility and the thermal behaviour of blends of microbial poly(D(−)3-hydroxybutyrate) (PHB) with atactic poly(methyl methacrylate) (aPMMA) have been investigated previously[1,2]. For a composition range varying from 90/10 to 10/90 PHB/aPMMA, the two components were found to be miscible at temperatures higher than 180°C, except for the 80/20 PHB/aPMMA composition. This blend was probably still not completely mixed at 200°C; higher temperatures could not be investigated owing to the thermal degradation of PHB. For a range of blend compositions varying from 70/30 to 20/80 PHB/aPMMA, upper critical solution temperature behaviour was evidenced at temperatures below 180°C; the phase behaviour was reversible and mixing and demixing processes were very fast, and consequently the crystallization from the melt state only occurred after demixing of the blend components. Amorphous blends, obtained by quenching, showed a single glass transition event, and the dependence of the glass transition temperature (T_g) on the composition was interpreted by using the free volume theory of Kovacs[3,4]. The obtained results suggested that quenched PHB/aPMMA blends form a homogeneous amorphous phase.

In the present paper the structure of cold-crystallized PHB/aPMMA blends is investigated with the aid of small-angle X-ray scattering (SAXS) and wide-angle X-ray diffraction (WAXD) techniques.

Experimental

Materials. PHB (Zeneca Bioproducts; $\bar{M}_w = 166000$, $\bar{M}_w/\bar{M}_n = 2.85$), a semicrystalline powder isolated from *Alcaligenes eutrophus* cultures, was blended with aPMMA (BDH; $\bar{M}_w = 116000$), with weight ratios of 70/30, 60/40 and 50/50 PHB/aPMMA. The binary blends were prepared by solution-casting from chloroform and were then dried under vacuum at 70°C until they reached constant weight.

Thin films of pure PHB and blends, sandwiched between microscope cover glasses, were melted at 185°C for 1 min and then quenched in an ice–water mixture. The quenched samples were cold-crystallized for 30 min, in an automatic hot-stage Mettler model FP-82 controlled by Mettler FP-80 Control Processor, at the temperatures reported in *Table 1*. For each blend composition the temperature of crystallization (T_c) was chosen to be 10°C lower than the temperature corresponding to the maximum of the exothermic crystallization peak observed during d.s.c. scans of quenched samples (see *Figure 1* in 'Results and discussion'). The time and T_c values ensured a complete and reproducible isothermal crystallization process for pure PHB and blends.

Scanning electron microscopy. Morphological analysis by scanning electron microscopy (SEM) was carried out on samples of pure PHB and blends hand-fractured after immersion in liquid nitrogen. The fractured surfaces were observed after gold-coating by using a Philips SEM model 515.

Table 1 Temperatures adopted for isothermal cold-crystallization (T_c), apparent melting temperatures (T'_m), crystalline weight fractions (X_c), crystallinities of PHB component ($X_{c(PHB)}$) and apparent crystal sizes (D_{020}), for pure PHB and PHB/aPMMA blends

PHB/aPMMA	T_c (°C)	T'_m (°C)	X_c [a]	$X_{c(PHB)}$	D_{020} (Å) [b]
100/0	42	174	0.50	0.50	185
70/30	62	173	0.34	0.49	185
60/40	82	171	0.31	0.51	165
50/50	103	169	0.29	0.58	145

[a] The errors in the X_c values were calculated as ±4%
[b] The errors in the D values were calculated as ±5 Å

*To whom correspondence should be addressed

0032-3861/94/13/2884-04

Differential scanning calorimetry. Quenched pure PHB and blends were analysed by a Perkin–Elmer DSC-4/Thermal Analysis Data Station from −50 to 200°C at a scanning rate of 20°C min^{-1}. About 10 mg of polymer, contained in a d.s.c. pan, was melted at 185°C for 1 min, quenched in an ice–water mixture and then rapidly transferred in the d.s.c. The T_g values were taken at the temperature corresponding to the maximum of the peak obtained by the first-order derivative of d.s.c. transition traces. The crystallization and observed melting temperatures were obtained from the maximum of the exothermic and endothermic peaks, respectively. D.s.c. scans were also conducted on cold-crystallized samples at the scanning conditions described above. Gallium and indium standard samples were used to calibrate the instrument.

Wide-angle X-ray diffraction. X-ray diffraction measurements were made on a Siemens diffractometer model D-500 equipped with a Siemens FK 60-10, 2000 W Cu tube (CuKα_1 radiation, $\lambda = 1.54$ Å). The degree of crystallinity was calculated from diffracted intensity data in the range $2\Theta = 11$–$40°$ by using the area integration method[5]. The method required that 100% amorphous polymer be available, then the diffracted intensity data of plain PHB and blends (quenched in an ice–water mixture) were collected at the measuring temperature of 8 ± 1°C and used to calculate the amorphous contribution. Lattice imperfections were not considered. The apparent crystal sizes were calculated from the line-broadening data collected with a scanning rate of 0.1 2Θ deg min^{-1}. A nickel standard sample was employed to determine the instrumental broadening.

Small-angle X-ray scattering. SAXS data were measured at 25°C using a Huber 701 chamber[6] with a monochromator glass block. Monochromatized CuKα_1 X-rays ($\lambda = 1.54$ Å) were supplied by a stabilized Siemens Kristalloflex 710 generator and a Siemens FK 60-04, 1500 W Cu target tube. The data were collected following a procedure previously described[7].

By application of the indirect transformation method developed by Glatter[8,9], the one-dimensional correlation function together with the corresponding propagated statistical error band were calculated from unsmoothed and smeared experimental scattering data. For the desmearing the geometries of the incident beam profile and of the detector were considered[8,10].

Results and discussion

Differential scanning calorimetry. *Figure 1* shows d.s.c. scans for pure PHB and PHB/aPMMA blends quenched in an ice–water mixture. The d.s.c. curves show the baseline shift corresponding to a single glass transition event followed by cold-crystallization and melting. For the 70/30, 60/40 and 50/50 PHB/aPMMA blends, the glass transition event is slightly shifted to higher temperatures with increasing aPMMA content. It can also be noted that the presence of the aPMMA component strongly increases the temperature of cold-crystallization of PHB.

The apparent melting temperature (T'_m) (*Table 1*) of the cold-crystallized samples decreases with increasing aPMMA content, although the samples were cold-crystallized at T_c values that increased with blending (*Table 1*). This fact is a preliminary indication that

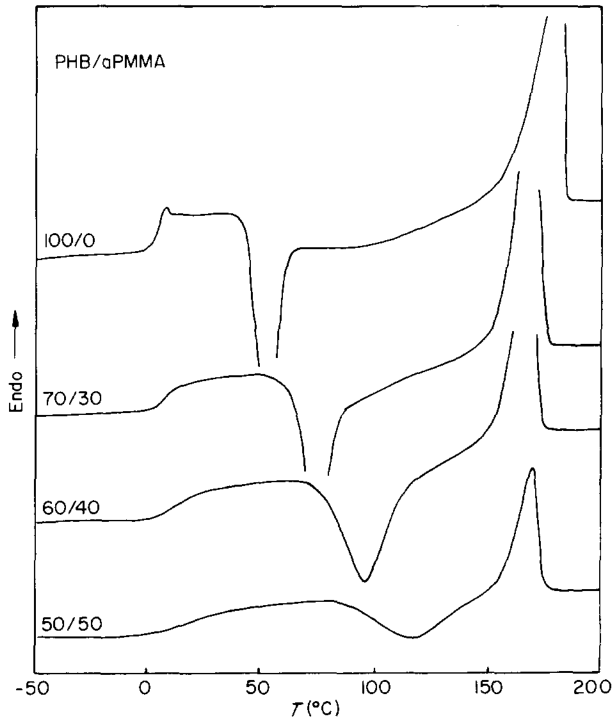

Figure 1 D.s.c. scans of quenched pure PHB and PHB/aPMMA blends

aPMMA can act as a diluent for PHB at the considered blend compositions.

Optical and scanning electron microscopy. Thin films of quenched pure PHB and PHB/aPMMA blends, when observed under the optical polarizing microscope, appeared homogeneous and without any birefringent region. After complete cold-crystallization at the temperatures reported in *Table 1*, the pure PHB and PHB/aPMMA blends appeared to be completely filled with impinged birefringent spherulites and no separated aPMMA domains were observed.

Examinations by SEM of liquid-nitrogen-fractured cold-crystallized blends revealed a homogeneous surface, and no domains of a separated phase were observed.

Wide-angle X-ray diffraction. In *Figure 2* the WAXD profiles of cold-crystallized pure PHB and 50/50 PHB/aPMMA blend are reported. The WAXD patterns correspond to the crystal structure of PHB homopolymer, which is known from previous work[11,12]. Measurements of d spacing of pure PHB and blends from the X-ray diffraction patterns showed constant values for the (1 1 0), (0 0 2) and (0 2 0) crystallographic planes, indicating that the PHB unit cell is unchanged in the blends.

The intensity of the crystalline peaks decreased with blending while the amorphous area, which includes the contribution of the amorphous PHB continuous scattering and of the aPMMA fraction, increased. The data reported in *Table 1* show that the crystallinity value of the PHB/aPMMA blends (X_c) decreases with increasing aPMMA content, while the crystallinity of the PHB component ($X_{c(PHB)}$) is similar for pure PHB and for 70/30 and 60/40 PHB/aPMMA blends, and higher for the 50/50 blend.

In *Table 1* the apparent crystal size values of pure and blended PHB are also reported; they were calculated by

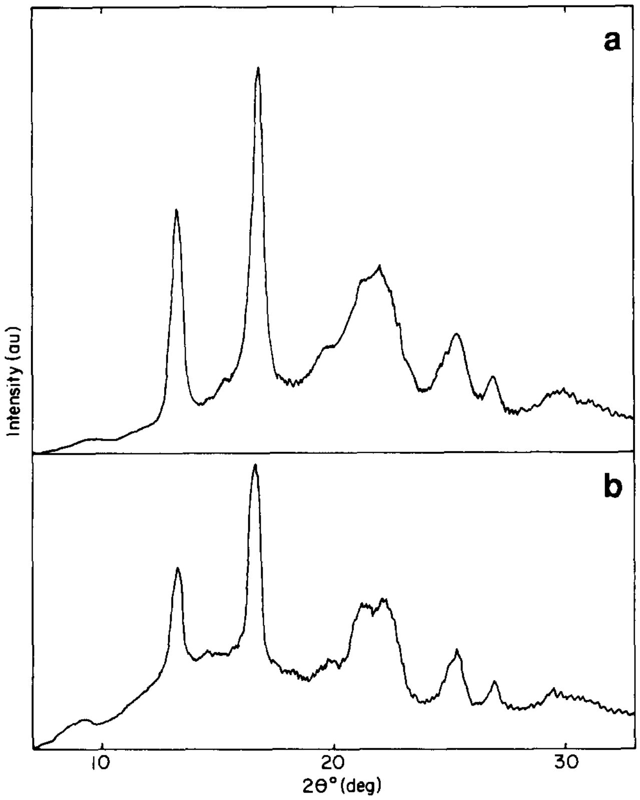

Figure 2 Wide-angle X-ray diffraction profiles of (a) cold-crystallized pure PHB and (b) cold-crystallized 50/50 PHB/aPMMA blend

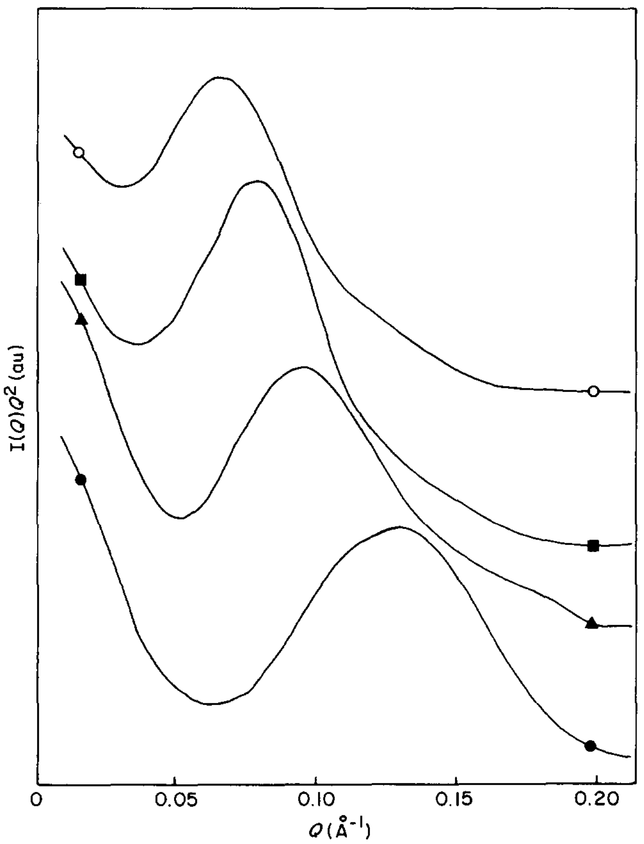

Figure 3 Desmeared and Lorentz-corrected intensity profiles of cold-crystallized PHB/aPMMA blends: ●, 100/0; ▲, 70/30; ■, 60/40; ○, 50/50

Table 2 Long period from experimental data (L) and long period calculated assuming all aPMMA to be in the interlamellar regions (L_{cal})

PHB/aPMMA	L (Å)	L_{cal} (Å)
100/0	51 ± 2	51
70/30	67 ± 2	74
60/40	81 ± 3	86
50/50	100 ± 3	104

the Sherrer equation[5] in the direction perpendicular to the (0 2 0) crystallographic plane (D_{020}).

Small-angle X-ray diffraction. The scattering profiles of cold-crystallized pure PHB and PHB/aPMMA blends show the presence of a maximum, which is associated with the long period (L) resulting from the presence of macrolattice formed by centres of adjacent lamellae.

Figure 3 reports the desmeared and Lorentz-corrected intensity profiles *versus* the abscissa variable Q ($Q = 4\pi(\sin\Theta)/\lambda$) for pure PHB and PHB/aPMMA blends; the maximum position shifts towards lower Q values with increasing aPMMA content in the blend. The L values were calculated by:

$$L = 2\pi/Q_m \tag{1}$$

where Q_m is the abscissa value at the maximum of the plot. The L values (*Table 2*) increase with increasing aPMMA content.

The one-dimensional correlation function $\gamma(r)$ was calculated for pure PHB and PHB/aPMMA blends, by the expression:

$$\gamma(r) = \frac{(1/\pi)\int_0^\infty I_t(Q)\cos(Qr)\,dQ}{(1/\pi)\int_0^\infty I_t(Q)\,dQ} \tag{2}$$

The model used to describe the scattering from a lamellar structure is the lamellar pseudo-two-phase structure discussed by Vonk[13,14]. This structure is defined as consisting of alternating parallel crystalline and amorphous lamellae connected by transition layers, where the variation of the electron density is assumed to be linear.

As can be observed in *Figure 4*, the correlation functions broaden on addition of aPMMA while the maximum shifts towards higher r values. No well-defined horizontal region is observed in the first minimum of the one-dimensional correlation function, because the wings of the first maximum cover part of the minimum[15]. The $\gamma(r)$ function and the crystallinity values obtained by WAXD were used to calculate the average amorphous and average crystalline thicknesses, $\langle A \rangle_n$ and $\langle C \rangle_n$, respectively, and the transition layer, $\langle E \rangle_n$ (refs 16 and 17). As reported in *Figure 5*, the thickness of the crystalline layer of the blends is quite constant and is higher than that of pure PHB, while the value of $\langle E \rangle_n$ is similar for pure PHB and blends. The interlamellar distance, $\langle A \rangle_n$, increases with blending, indicating that the aPMMA is segregated in the PHB interlamellar regions.

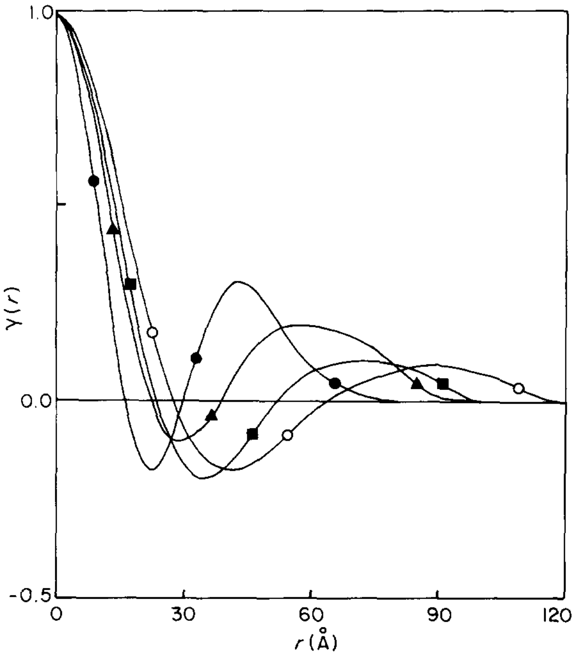

Figure 4 One-dimensional correlation function, $\gamma(r)$, of cold-crystallized PHB/aPMMA blends: ●, 100/0; ▲, 70/30; ■, 60/40; ○, 50/50

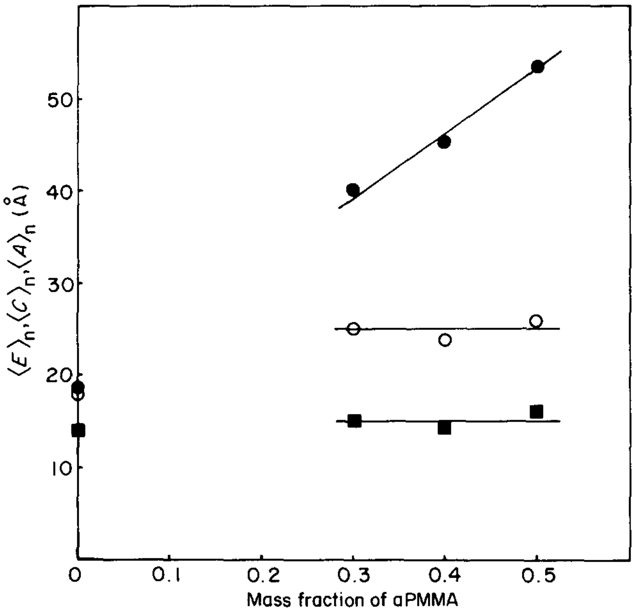

Figure 5 Average amorphous interlamellar thickness $\langle A\rangle_n$ (●), average crystalline thickness $\langle C\rangle_n$ (○) and average interphase thickness $\langle E\rangle_n$ (■), *versus* blend composition

According to a two-phase model, if all aPMMA were in the interlamellar regions, the value of the long period of PHB/aPMMA blends, L_{cal}, could be estimated, assuming volume additivity, by the following relation:

$$L_{cal} = L_{(PHB)}/V_2 \quad (3)$$

where V_2 is the volume fraction of the crystallizable material in the blends and $L_{(PHB)}$ is the experimental long period of the pure PHB. The values of L_{cal} reported in *Table 2* are in good agreement with the experimental values, confirming that during PHB cold-crystallization the aPMMA component is totally segregated in the amorphous PHB interlamellar regions.

To explain the scale of segregation of aPMMA in the PHB cold-crystallizing matrix, the Keith and Padden equation[18] could be used, i.e. $\delta = D/G$. This expression places the scale of segregation on a somewhat quantitative basis; δ is the dimensional order of segregation, D is the diffusion coefficient of the non-crystallizing component in the crystallizing matrix, and G is the spherulitic radial growth rate. The parameter δ has dimensions of length and represents the distance that the rejected component may move during the time of crystallization. If δ is comparable with interlamellar distances, then the rejected component may reside between lamellae. In the case of PHB/aPMMA blends, qualitatively, the amorphous component has considerably higher T_g than the crystallizing polymer, and therefore the addition of aPMMA greatly decreases the diffusion term such that segregation can occur at the lamellar level.

Conclusions

The melt-miscible PHB/aPMMA blends show a demixing phenomenon when undercooled from the melt state to the temperature of PHB crystallization. In contrast, with the quenching procedure adopted in this work, the cold-crystallization of PHB from a homogeneous mixture is possible. The experimental results show that during isothermal cold-crystallization of PHB/aPMMA blends, the non-crystallizable aPMMA component is segregated in the amorphous PHB interlamellar regions. In fact the thickness of the amorphous interlamellar zones and the long period distance increase with increasing aPMMA content.

References

1 Siciliano, A., Seves, A., De Marco, T., Cimmino, S., Martuscelli, E. and Silvestre, C. Fourth European Symposium on Polymer Blends, Capri, May 1993, book of abstracts, p. 90
2 Siciliano, A., Seves, A., De Marco, T., Cimmino, S., Silvestre, C. and Martuscelli, E., in preparation
4 Aubin, M. and Prud'homme, R. E. *Macromolecules* 1988, **21**, 2945
5 Alexander, L. E. 'X-ray Diffraction Method in Polymer Science', Wiley-Interscience, New York, 1969, p. 137
6 Schnabel, E., Hosemann, R. and Rode, B. *J. Appl. Phys.* 1972, **43**, 3237
7 Sadocco, P., Canetti, M., Seves, A. and Martuscelli, E. *Polymer* 1993, **34**, 3369
8 Glatter, O. and Krakty, O. 'Small Angle X-ray Scattering', Academic Press, London, 1982, p. 119
9 Glatter, O. *J. Appl. Cryst.* 1980, **13**, 577
10 Glatter, O. *J. Appl. Cryst.* 1977, **10**, 415
11 Bluhm, T. L., Hamer, G. K., Marchessault, R. H., Fyfe, C. A. and Veregin, R. P. *Macromolecules* 1986, **19**, 2871
12 Kunioka, M., Tamaki, A. and Doi, Y. *Macromolecules* 1989, **22**, 694
13 Vonk, C. G. *J. Appl. Cryst.* 1973, **8**, 81
14 Vonk, C. G. and Kortleve, G. *Koll. Z. Z. Polym.* 1967, **220**, 19
15 Vonk, C. G. and Pijpers, A. P. *J. Polym. Sci., Polym. Phys. Edn* 1985, **23**, 2517
16 Silvestre, C., Karasz, F. E., MacKnight, W. J. and Martuscelli, E. *Eur. Polym. J.* 1987, **23**, 745
17 Silvestre, C., Cimmino, S., Martuscelli, E., Karasz, F. E. and MacKnight, W. J. *Polymer* 1987, **28**, 1190
18 Keith, H. D. and Padden, F. J. *J. Appl. Phys.* 1964, **35**(4), 1270